Carbohydrate Polymers 102 (2014) 956–961

Contents lists available at ScienceDirect

Carbohydrate Polymers

journal homepage: www.elsevier.com/locate/carbpol

Photocatalytic activities of cellulose-based nanofibers with different silver phases: Silver ions and nanoparticles

Ki Hyuk Jang[a], Yun Ok Kang[b], Taek Seung Lee[a], Won Ho Park[a,*]

[a] Department of Advanced Organic Materials and Textile System Engineering, Chungnam National University, Daejeon 305-764, South Korea
[b] Department of Nanotechnology, Chungnam National University, Daejon 305-764, South Korea

ARTICLE INFO

Article history:
Received 11 August 2013
Received in revised form
26 September 2013
Accepted 12 October 2013
Available online 4 November 2013

Keywords:
Cellulose
Silver
Nanofibers
Catalyst

ABSTRACT

Cellulose acetate (CA) nanofibers with 5 wt% $AgNO_3$ were fabricated by electrospinning. The Ag ions in as-spun CA nanofibers were photo-reduced to Ag nanoparticles (NPs) using a UV irradiation, and the UV-irradiated CA nanofibers were then transformed to cellulose nanofibers containing Ag NPs by deacetylation reaction. The size and content of Ag NPs in CA fibers was further increased under the deacetylation condition. The catalytic activity of the CA and cellulose nanofibers with different Ag ions/NPs ratios was examined by two model reactions; photodegradation reaction of methylene blue (MB) and chemiluminescent (CL) reaction of luminol. The Ag ions played an important role as a reducing catalyst of MB, whereas the Ag NPs are more effective than Ag ions in the CL reaction. Therefore, the CA and cellulose nanofibrous matrices with Ag ions or NPs have diverse potential applications as catalytic membranes for sensing to specific chemicals.

1. Introduction

With the development of nanofabrication techniques, considerable attention has been paid to nanostructures, such as nanofibers and nanoparticles (Lara, Garza-Treviño, Ixtepan-Turrent, & Singh, 2011; Sundarrajan & Ramakrishna, 2010). Polymer nanofibers, which exhibit outstanding properties including a high specific surface area and a high porosity, can be used for a wide variety of applications, such as separation filters, wound dressing materials, scaffolds for tissue engineering, sensors, etc. (Li & Xia, 2004). Metal nanoparticles (NPs) also display special mechanical, electrical, optical, magnetic, thermal and catalytic properties (Lok et al., 2006). Among metal NPs, a large number of studies have been conducted on silver (Ag) NPs, due to its ease of formation. Ag NPs are of particular interest due to their good conductivity, chemical stability, and catalytic and antibacterial activity (Panáček et al., 2009). In addition, Ag NPs can be easily incorporated into polymer matrices, including polymer nanofibers. The incorporation of Ag NPs into a nanofibrous structure is an attractive hybridization method because Ag NPs distributed evenly in the nanofibrous structure can be used for novel specific applications in catalysis, sensors, photonics, and electronics (Cozza, Monticelli, & Marsano, 2010; Demir et al., 2004; Kedem, Schmidt, Paz, & Cohen, 2005; Lu, Zhao, Wang, & Wei, 2005; Zhao, Sun, Lv, & Li, 2012). A combination of Ag NPs and polymer nanofibers can be accomplished by electrospinning the polymer solution containing Ag NPs or Ag salts, which are then reduced into NPs in the electrospun polymer nanofibers. The advantage of Ag-incorporated polymer nanofibers are that the polymer nanofibers improve the dispersing ability by limiting the aggregation of Ag, and thus their applications are extended to novel specific fields, whereby the Ag NPs alone are not able to efficiently demonstrate their outstanding functions. The functional properties of these polymer nanocomposites are strongly dependent on the content, size, distribution and structure of the Ag NPs that are incorporated within them.

In the previous studies (Son, Youk, Lee, & Park, 2004; Son, Youk, & Park, 2006), cellulose acetate (CA) nanofibers containing Ag NPs were prepared by photoreducing Ag^+ ions within the CA nanofibers electrospun from a CA solution with small amounts of $AgNO_3$. The Ag NPs were stabilized by their interactions with the carbonyl oxygen atoms in the CA and exhibited very strong antimicrobial activity. In this study, the CA and cellulose nanofibers with different Ag ions/NPs ratios were fabricated by electrospinning, UV irradiation and deacetylation under KOH/ethanol solution (Scheme 1). The catalytic activities of the cellulose-based nanofibrous matrix with different Ag phases (ions or NPs) were examined by two model reactions: reduction reaction of methylene blue (MB) and chemiluminescent (CL) reaction of luminol.

* Corresponding author. Tel.: +82 42 821 6613; fax: +82 42 823 3736.
E-mail address: parkwh@cnu.ac.kr (W.H. Park).

0144-8617/$ – see front matter © 2013 Elsevier Ltd. All rights reserved.
http://dx.doi.org/10.1016/j.carbpol.2013.10.036

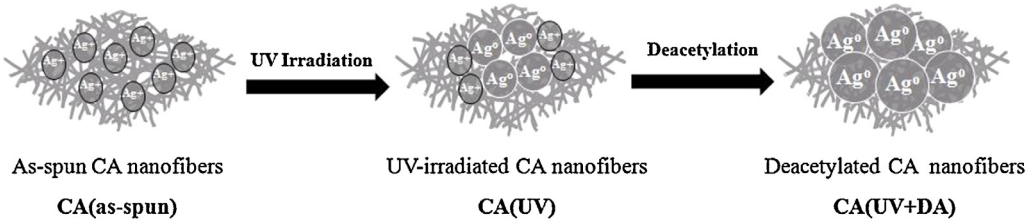

Scheme 1. Preparation procedure of cellulose nanofibers containing Ag nanoparticles.

2. Experimental

2.1. Materials

CA (acetyl content 39.8%, M_W = 30,000) and silver nitrate ($AgNO_3$) were obtained from Aldrich Co. and used without further purification. Glacial acetic acid, ethanol, potassium hydroxide (KOH), methylene blue (MB, 98.5%), luminol (98.0%), sodium borohydride ($NaBH_4$), hydrogen peroxide (H_2O_2, 30%), 0.1 N sodium hydroxide (NaOH), and sodium carbonate (Na_2CO_3) were purchased from commercial suppliers and used as received without further purification.

2.2. Electrospinning

In order to fabricate the CA nanofibers containing Ag^+ ions, CA and $AgNO_3$ were dissolved in a mixed solvent of acetic acid/water (75/25, w/w). The concentrations of CA and $AgNO_3$ were 16 wt% and 5.0 wt%, respectively. The weight percentage of $AgNO_3$ was calculated on the basis of the weight of CA. The electrospinning setup consisted of a syringe and needle (ID = 0.84 mm), an aluminum collecting plate, and a high voltage supply (Chungpa EMT). A syringe pump connected to the syringe controlled the flow rate. The CA solutions were electrospun at a positive voltage of 25 kV, a working distance of 10 cm (the distance between the needle tip and the collecting plate), and a solution flow rate of 0.3–3 mL/h.

2.3. Photoreduction of Ag^+ ions in the CA nanofibers

For the photoreduction of Ag^+ ions in the CA nanofibers, the as-spun CA nanofibers were irradiated with UV light having a maximum wavelength of 254 nm for 0–4 h, using a 500 W high-pressure Hg lamp system (StabiLight, NT-LS-HG50-SR).

2.4. Deacetylation of CA nanofibers

The irradiated CA nanofibers (0.25 g) were deacetylated with 12.5 mL of 0.5 N KOH in ethanol at 25 °C for 30 min and then washed several times with deionized water.

2.5. Catalytic activity

The catalytic activity of Ag in the CA and cellulose nanofibers was examined as follows: The nanofiber webs containing 5 wt% Ag (1 mg) was placed into a MB solution in water (2.475 mL, 0.01 mol/L), and an aqueous $NaBH_4$ solution (0.025 mL, 0.1 mol/L) under constant stirring was then added. The reduction reaction of MB catalyzed by Ag was monitored with a UV-visible spectrophotometer (Shimadzu UV2450, Japan).

Chemiluminescence (CL) of luminol by Ag in the CA and cellulose nanofibers was examined as follows: The nanofiber webs containing 5 wt% Ag (3 mg) was placed into the luminol solution (2 mL, 0.1 mol/L), and a diluted H_2O_2 solution (0.2 mL) under constant stirring was then added. The chemiluminescence (CL) detection was monitored with a Perkin Elmer LS45 spectrofluorometer or FL 5401spectrofluorometer (Shimadzu, Japan).

2.6. Measurements and characterization

The morphology of as-spun, irradiated and deacetylated CA nanofibers containing Ag was observed on a field emission scanning electron microscope (FE-SEM; JSM-7000F, JEOL, Japan). The average diameter and diameter distribution were obtained by analyzing SEM images using a custom code image analysis program (Scope Eye II, Masan, Korea). TEM images were obtained using a Philips CM 200 transmission electron microscope for samples deposited on carbon coated copper grids. The crystalline structure of the samples was analyzed on a wide-angle X-ray

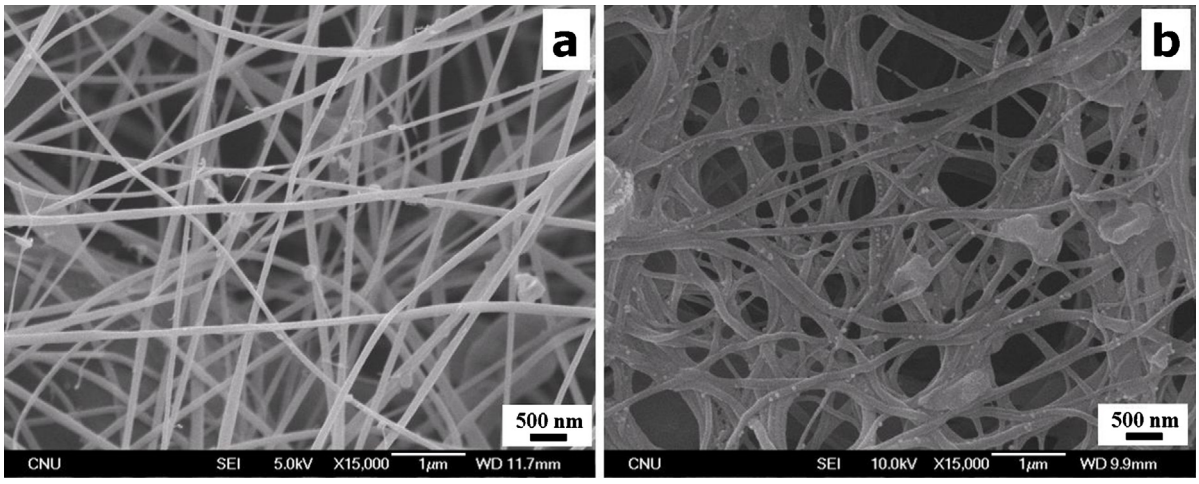

Fig. 1. SEM images of as-spun (a) and deacetylated (b) CA nanofibers containing 5 wt% Ag.

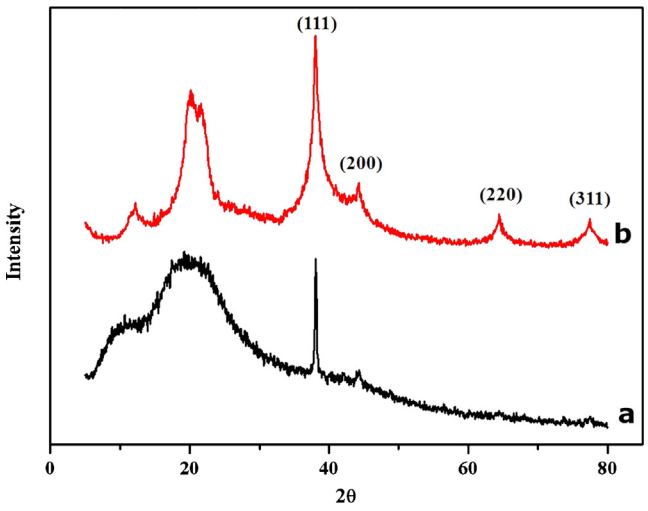

Fig. 2. XRD patterns of UV-irradiated (a) and deacetylated (b) CA nanofibers with Ag ions/NPs.

diffractometer (model D/max-IIB, Rigaku International Corp., Japan). The XPS spectra of the nanofibrous matrices were recorded on a VG Escalab Mk2 spectrometer equipped with an unmonochromatized Mg Kα X-ray source (1253.6 eV) and hemispherical analyzer (Korea Basic Science Institute). High resonance XPS spectra were recorded in 0.05 eV steps with a pass energy of 20 eV. The binding energy peaks were deconvoluted using Gaussian functions and a least squares curve-fitting program.

3. Results and discussion

In the previous study (Han, Youk, Min, Kang, & Park, 2008) [13], an optimum solvent mixture of acetic acid/water (75/25, w/w) was newly developed for the feasible electrospinning of a CA solution. Fig. 1 shows SEM images of as-spun and deacetylated CA nanofibers containing 5 wt% Ag using a solvent mixture of acetic acid/water. The average diameter (80 nm) of the as-spun CA nanofibers containing $AgNO_3$ was considerably smaller than that of the pure CA nanofibers (330 nm) without $AgNO_3$. The addition of $AgNO_3$ increased the charge density in the CA solutions and thus stronger elongational forces were imposed on the ejected jets under the electrical field, resulting in a substantially straighter shape and finer CA nanofibers.

Ag NPs in the nanofibers can be prepared by photoreduction using a UV irradiation (Díez, Hahn, Ikkala, Börner, & Ras, 2010; Pant, Pandeya, Nam, Baek, Hong, & Kim, 2011; Sui et al., 2012). When the CA nanofibers with $AgNO_3$ were irradiated with UV light at 254 nm for 4 h, the color of as-spun CA nanofibers gradually changed to brown with increasing the irradiation time up to 4 h, indicating that Ag ions in the CA nanofibers were rapidly photoreduced and aggregated into Ag NPs. Ag NPs were formed preferentially on the surface of the CA nanofibers and had an almost spherical shape (Son et al., 2006).

The UV-irradiated CA nanofibers were deacetylated in a 0.5 N KOH/ethanol solution for 30 min. The changes in the chemical structure of the CA nanofibers during deacetylation were analyzed using FT-IR spectroscopy. After 30 min, the characteristic adsorption peak of CA at 1745 cm^{-1} (ν_{C-O}) completely disappeared, indicating that the CA nanofibers were converted into cellulose nanofibers. The morphological structure of the CA nanofibers was well maintained after deacetylation, even though the deacetylated CA (cellulose) nanofibers showed a slightly swollen morphology (Fig. 1b).

Fig. 2 shows XRD patterns of UV-irradiated and deacetylated CA nanofibers with Ag ions/NPs. After deacetylation, a broad peak ($2\theta = 5–25^\circ$) attributed to the crystalline structure of CA molecules disappeared, and the intensity of the peak ($2\theta = 22^\circ$) corresponding to the crystalline structure of cellulose molecules was increased. In the UV-irradiated CA nanofibers, the four distinct XRD peaks were not observed clearly at 2θ values of 38.2, 44.5, 64.6, and 77.5, corresponding to the reflections of the (1 1 1), (2 0 0), (2 2 0), and (3 1 1) crystalline planes of the metallic face-centered cubic Ag, respectively. This demonstrates that the Ag ions in the CA nanofibers were not converted completely to the Ag NPs. On the other hand, the four distinct XRD peaks by the Ag crystalline structure could be observed clearly in the deacetylated CA (cellulose) nanofibers. This suggests that the amount and size of the Ag NPs in the deacetylated CA nanofibers was further increased by deacetylation under an alkaline KOH condition. Further increase in the amount and size of Ag NPs during deacetylation may be explained by reducing the action of ethanolic KOH solution on Ag NPs. Ethanol is a reducing agent used to generate the Ag NPs (Kim, 2007; Kim, Kim, Veriansyah, Won Kang, & Kim, 2009). Furthermore, the ethanol in alkaline (KOH) condition had a higher reducing power to Ag ions or NPs (Chou, Lu, & Lee, 2005). Thus, the Ag ions or NPs in the CA nanofibers grouped together and formed larger NPs during deacetylation reaction.

The composition of Ag ions and NPs in the CA nanofibers was determined by XPS. Fig. 3 shows XPS spectra of Ag regions for CA nanofibers with different Ag ions/NPs. As shown in Fig. 3a, as-spun CA nanofibers with Ag^+ ions showed the doublet peaks at 367.4 and 373.4 eV, corresponding to Ag $3d_{5/2}$ and Ag $3d_{3/2}$ binding energies, respectively. On the other hand, the deacetylated CA nanofibers with Ag NPs showed the doublet peaks at 367.8 and 373.8 eV (Fig. 3c). The Ag $3d_{5/2}$ and Ag $3d_{3/2}$ binding energies at 367.4 and 373.4 eV, corresponding to Ag^+ ions, were shifted slightly to higher binding energies of 367.8 and 373.8 eV corresponding to metallic Ag^0 (Kang & Sohn, 2012). This shift indicates that the Ag ions were transformed to Ag NPs (Luong, Lee, & Nam, 2008). On the other hand, the UV-irradiated CA nanofibers showed broad intermediate doublet peaks, although their maximums appeared at approximately 367.8 and 373.8 eV (Fig. 3b). The peak deconvolution reveals the presence of a second component displaced in 0.4 eV toward a lower binding energy, which can be easily identified as Ag^+ ions. Therefore, the relative contents (%) of Ag ions and NPs were obtained by curve fitting, as listed in Table 1. The Ag atoms in the UV-irradiated CA nanofibers were composed of ~66% Ag NPs and ~34% Ag ions.

The catalytic activity of the CA nanofibers with different Ag ions/NPs ratios was examined using two model reactions: reduction (photodegradation) reaction of MB and chemiluminescent reaction of luminol. The catalytic activity of the Ag ions/NPs in the CA nanofibers was investigated using a reduction reaction between MB dye and a reducing agent $NaBH_4$. MB has a characteristic absorption peak at 668 nm. The intensity of the absorption at 668 nm is proportional to the concentration of MB in the medium. The catalytic activity of the CA nanofibers was carried out by reduction of 2.475 mL of MB (0.01 mol/L) in water using

Table 1
Morphological parameters of as-spun, UV-irradiated and deacetylated CA nanofibers.

Sample	AFD[a] (nm)	Total Ag content (wt%)	Relative Ag^+ ion content (%)	Relative Ag nanoparticle content (%)	Ag nanoparticle size (nm)
CA (as-spun)	80	5	100	0	–
CA (UV)	80	5	34	66	15
CA (UV + DA[b])	95	5	0	100	56

[a] AFD: average fiber diameter.
[b] DA: deacetylated.

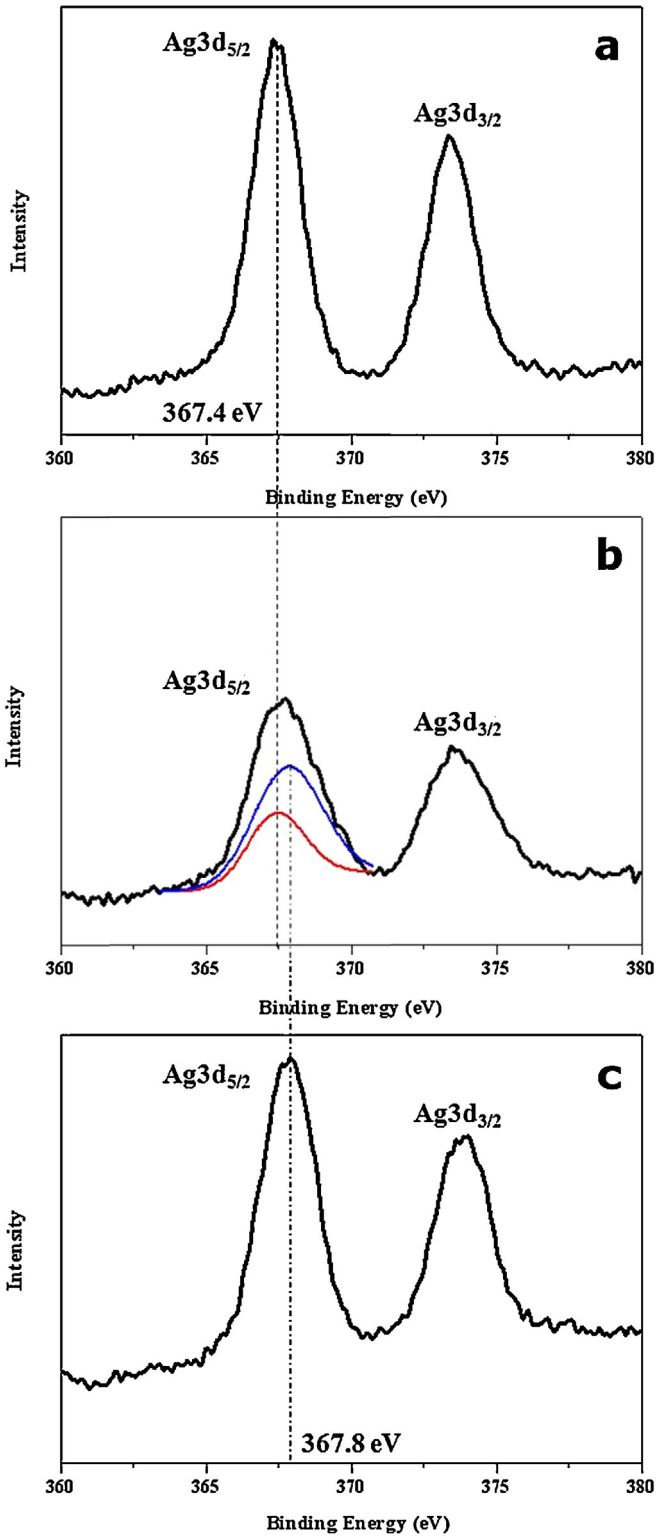

Fig. 3. XPS spectra of Ag regions for CA nanofibers with different Ag ions/NPs; (a) as-spun CA nanofibers, (b) UV-irradiated CA nanofibers, (c) deacetylated CA nanofibers.

1 mg CA nanofibers containing 5 wt% Ag ions/NPs as an catalyst and 0.025 mL of $NaBH_4$ (0.1 mol/L) as a reducing agent. The progression of the catalytic reduction of MB can be easily followed by the change in optical density at the λ_{max} of 668 nm. Evidently, the absorbance at λ_{max} of 668 nm gradually decreased with reaction time, together with the color change from blue to colorless (Fig. 4a).

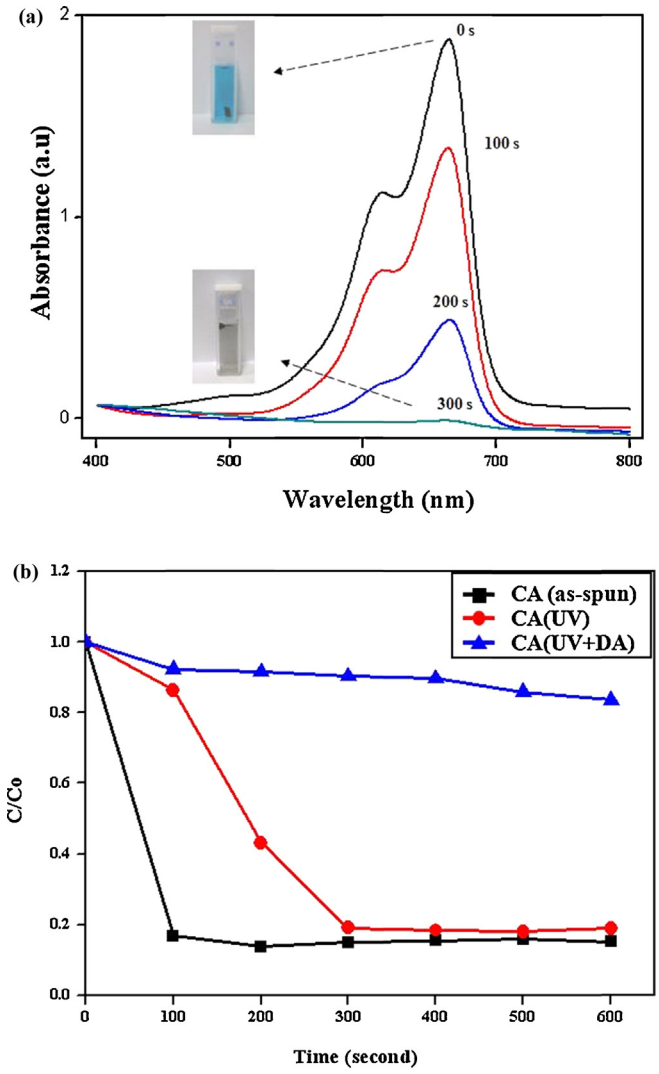

Fig. 4. (a) Change in the absorbance at λ_{max} of 668 nm of MB solution with reaction time, and (b) the reduction rate (C/C_0) of MB under the CA nanofibers with different Ag ions/NPs.

The decrease in absorbance is probably due to the degradation of the MB chromophore (Kim, Cho, & Park, 2010). Therefore, the rate of degradation reaction can be determined by measuring the intensity of the absorbance of the MB solution at 668 nm. Fig. 4b shows the reduction rate (C/C_0) of MB under the CA nanofibers with different Ag ions/NPs. C_0 and C denote the concentration of MB at a UV irradiation time of 0 and t, respectively. The fastest reduction was obtained with the CA nanofibers with Ag ions. The reduction rate of MB was faster in the order of CA (as-spun) > CA (UV) > CA (UV + DA). In the as-spun and UV-irradiated CA nanofibers, MB degradation was almost completed at 100 and 300 s, respectively, whereas the degradation of MB nearly occurred with deacetylated CA nanofibers containing Ag NPs after 600 s. Therefore, the rate of MB degradation was strongly dependent on the Ag ion contents in the CA nanofibers. This result demonstrates that the Ag ions played an important role as a reducing catalyst of MB.

Chemiluminescence (CL) is a phenomenon that occurs when a vibronically excited product of an exoergic reaction relaxes back to its ground state with the emission of photons (Liu, Kou, Jiang, Zhang, & Qi, 2012). Luminol is a common CL reagent used in CL reaction. The luminol-H_2O_2 system plays an important role in modern chemical analysis. Fig. 5a shows the spectra of CL with the CA

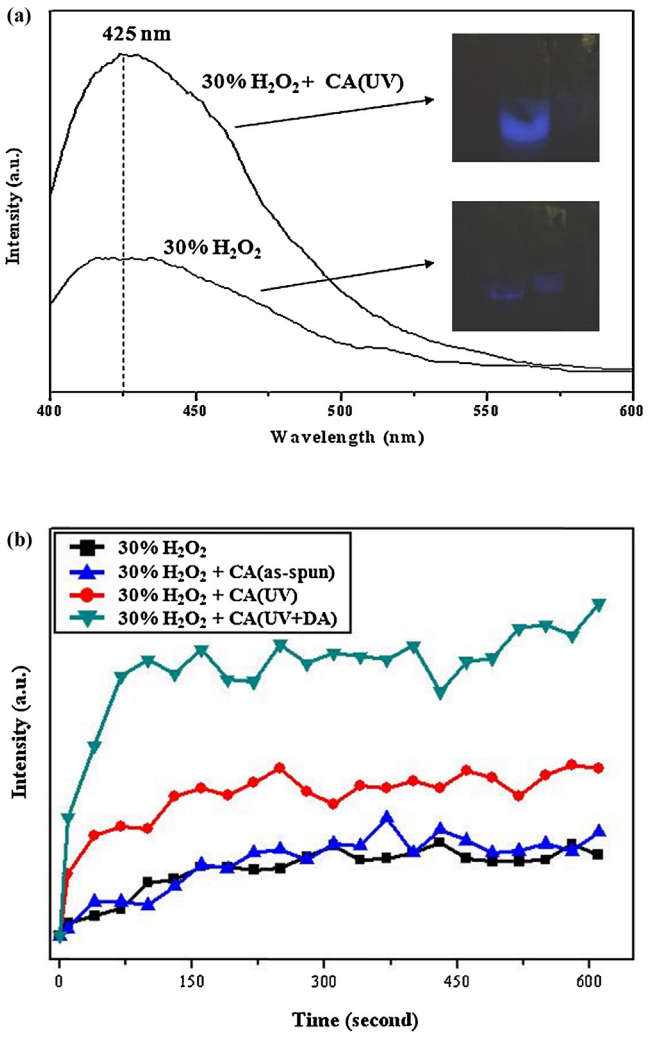

Fig. 5. (a) Spectra of CL with the CA nanofibers containing Ag ion/NPs, and (b) the relationship between CL intensity and reaction time in luminol-H_2O_2 system with the CA nanofibers containing different Ag ions/NPs (pH 11.4, 0.2 mmol/L luminal, 0.15 mol/L H_2O_2, and CA nanofibers 0.5 g).

nanofibers containing Ag ion/NPs, along with a control sample. The maximum emission wavelength of CL reaction was approximately 425 nm, which concurs with previous reports (Chandel, Khan, Kher, & Tiwari, 2012; Liu, Kou, Jiang, Zhang, & Qi, 2012; Xu & Cui, 2007). Fig. 5b shows the relationship between CL intensity and reaction time in the luminol-H_2O_2 system with the CA nanofibers containing different Ag ions/NPs (pH 11.4, 0.2 mmol/L luminal, 0.15 mol/L H_2O_2, and CA nanofibers 0.5 g). The CL intensity was stronger in the order of CA (UV + DA) > CA (UV) > CA (as-spun) > control, indicating that the Ag NPs was more effective in enhancing the CL reaction of luminol than Ag ions. This result can be explained by the suggested mechanism of gold, platinum and silver NPs. In this mechanism, the electron transfer reaction between the Ag NPs and H_2O_2 is an initiating step for the subsequent CL process ($Ag_n + H_2O_2 \rightarrow Ag_n^+ + \bullet OH + OH^-$).

4. Conclusion

The CA and cellulose nanofibers with different Ag ions/NPs ratios were fabricated by electrospinning, UV irradiation and deactylation under alkaline condition. The catalytic activity of the CA and cellulose nanofibers with different Ag ions/NPs ratios was examined using two model reactions; reduction reaction of MB and chemiluminescent reaction of luminol. The reduction rate of MB was higher in the order of CA (as-spun) > CA (UV) > CA (UV + DA). This result shows that Ag ions played an important role as a reducing catalyst of MB. On the contrary, the CL intensity was stronger in the order of CA (UV + DA) > CA (UV) > CA (as-spun), indicating that the Ag NPs is more effective than the Ag ions in the CL reaction. Therefore, the CA and cellulose nanofibrous matrices with Ag ions or NPs have diverse potential applications as catalytic membranes for sensing to specific chemicals.

Acknowledgement

This research was supported by Basic Science Research Program through the National Research Foundation of Korea (NRF) funded by the Ministry of Science, ICT & Future Planning (2012R1A1A2008761).

References

Chandel, A., Khan, S., Kher, R., & Tiwari, A. (2012). Investigation on the chemiluminescence reaction of the phenylhydrazine-luminol–peroxide system. *Luminescence*, *27*(6), 455–458.

Chou, K.-S., Lu, Y.-C., & Lee, H.-H. (2005). Effect of alkaline ion on the mechanism and kinetics of chemical reduction of silver. *Materials Chemistry and Physics*, *94*(2), 429–433.

Cozza, E. S., Monticelli, O., & Marsano, E. (2010). Electrospinning: A novel method to incorporate POSS into a polymer matrix. *Macromolecular Materials and Engineering*, *295*(9), 791–795.

Demir, M. M., Gulgun, M. A., Menceloglu, Y. Z., Erman, B., Abramchuk, S. S., Makhaeva, E. E., et al. (2004). Palladium nanoparticles by electrospinning from poly (acrylonitrile-co-acrylic acid)-PdCl2 solutions. Relations between preparation conditions, particle size, and catalytic activity. *Macromolecules*, *37*(5), 1787–1792.

Díez, I., Hahn, H., Ikkala, O., Börner, H. G., & Ras, R. H. (2010). Controlled growth of silver nanoparticle arrays guided by a self-assembled polymer–peptide conjugate. *Soft Matter*, *6*(14), 3160–3162.

Han, S. O., Youk, J. H., Min, K. D., Kang, Y. O., & Park, W. H. (2008). Electrospinning of cellulose acetate nanofibers using a mixed solvent of acetic acid/water: Effects of solvent composition on the fiber diameter. *Materials Letters*, *62*(4), 759–762.

Kang, J.-G., & Sohn, Y. (2012). Interfacial nature of Ag nanoparticles supported on TiO_2 photocatalysts. *Journal of Materials Science*, *47*(2), 824–832.

Kedem, S., Schmidt, J., Paz, Y., & Cohen, Y. (2005). Composite polymer nanofibers with carbon nanotubes and titanium dioxide particles. *Langmuir*, *21*(12), 5600–5604.

Kim, J.-S. (2007). Antibacterial activity of Ag^+ ion-containing silver nanoparticles prepared using the alcohol reduction method. *Journal of Industrial and Engineering Chemistry*, *13*(5), 718–722.

Kim, J., Kim, D., Veriansyah, B., Won Kang, J., & Kim, J.-D. (2009). Metal nanoparticle synthesis using supercritical alcohol. *Materials Letters*, *63*(21), 1880–1882.

Kim, Y. B., Cho, D., & Park, W. H. (2010). Fabrication and characterization of TiO_2/poly (dimethyl siloxane) composite fibers with thermal and mechanical stability. *Journal of Applied Polymer Science*, *116*(1), 449–454.

Lara, H. H., Garza-Treviño, E. N., Ixtepan-Turrent, L., & Singh, D. K. (2011). Silver nanoparticles are broad-spectrum bactericidal and virucidal compounds. *Journal of Nanobiotechnology*, *9*, 30.

Li, D., & Xia, Y. (2004). Electrospinning of nanofibers: Reinventing the wheel? *Advanced Materials*, *16*(14), 1151–1170.

Liu, W., Kou, J., Jiang, X., Zhang, Z., & Qi, H. (2012). Determination of nitrofurans in feeds based on silver nanoparticle-catalyzed chemiluminescence. *Journal of Luminescence*, *132*(4), 1048–1054.

Lok, C.-N., Ho, C.-M., Chen, R., He, Q.-Y., Yu, W.-Y., Sun, H., et al. (2006). Proteomic analysis of the mode of antibacterial action of silver nanoparticles. *Journal of Proteome Research*, *5*(4), 916–924.

Lu, X., Zhao, Y., Wang, C., & Wei, Y. (2005). Fabrication of CdS nanorods in PVP fiber matrices by electrospinning. *Macromolecular Rapid Communications*, *26*(16), 1325–1329.

Luong, N. D., Lee, Y., & Nam, J.-D. (2008). Highly-loaded silver nanoparticles in ultrafine cellulose acetate nanofibrillar aerogel. *European Polymer Journal*, *44*(10), 3116–3121.

Panáček, A., Kolář, M., Večeřová, R., Prucek, R., Soukupová, J., Kryštof, V., et al. (2009). Antifungal activity of silver nanoparticles against *Candida spp. Biomaterials*, *30*(31), 6333–6340.

Pant, H. R., Pandeya, D. R., Nam, K. T., Baek, W.-I., Hong, S. T., & Kim, H. Y. (2011). Photocatalytic and antibacterial properties of a TiO_2/nylon-6 electrospun nanocomposite mat containing silver nanoparticles. *Journal of Hazardous Materials*, *189*(1), 465–471.

Son, W. K., Youk, J. H., Lee, T. S., & Park, W. H. (2004). Preparation of antimicrobial ultrafine cellulose acetate fibers with silver nanoparticles. *Macromolecular Rapid Communications*, *25*(18), 1632–1637.

Son, W. K., Youk, J. H., & Park, W. H. (2006). Antimicrobial cellulose acetate nanofibers containing silver nanoparticles. *Carbohydrate Polymers*, *65*(4), 430–434.

Sui, C., Li, C., Guo, X., Cheng, T., Gao, Y., Zhou, G., et al. (2012). Facile synthesis of silver nanoparticles-modified PVA/$H_4SiW_{12}O_{40}$ nanofibers-based electrospinning to enhance photocatalytic activity. *Applied Surface Science*, *258*(18), 7105–7111.

Sundarrajan, S., & Ramakrishna, S. (2010). Fabrication of functionalized nanofiber membranes containing nanoparticles. *Journal of Nanoscience and Nanotechnology*, *10*(2), 1139–1147.

Xu, S. L., & Cui, H. (2007). Luminol chemiluminescence catalysed by colloidal platinum nanoparticles. *Luminescence*, *22*(2), 77–87.

Zhao, D. M., Sun, L. G., Lv, L. L., & Li, J. (2012). Preparation of cellulose acetate ultra-fine fibers containing quasi-spherical gold nanoparticles by electrospinning method. *Advanced Materials Research*, *391*, 400–403.